

An Effective Noise-Reduction Scheme for Microwave Amplifiers

S. Römisch¹ and F. Ascarrunz²
¹ScriptL, LLC ²Spectradynamics, Inc.
 1212 Louisville, CO 80027, USA
 Email: struzzo@americanisp.net

Abstract- An effective noise cancellation scheme, based on feedforward techniques after cancellation of the signal carrier, is presented. Experimental characterization of a proof-of-concept system applied to a 10GHz linear amplifier yielded up to 20dB of noise reduction for offset frequencies smaller than 100 kHz. The system described in this paper allows reducing both white and flicker noise.

A thorough analysis of the canceling mechanisms supports the measurement results and allows considerations of the limits of the scheme.

I. INTRODUCTION

Amplitude and phase noise in amplifiers are important in several fields including communications, timekeeping and frequency control. For oscillators in the microwave range and above, for example, it is well known that the noise performance limit is set by the amplifier noise, especially for $1/f$ -type of noise processes (see for example [1]). This noise type is mainly generated through a multiplicative process and consequently very difficult to eliminate. The signal-to-noise ratio cannot be improved by increasing the power in the signal carrier. Noise cancellation techniques reduce many kinds of noise processes and affect both amplitude and phase noise because they operate on the amplitude of noise sidebands.

The scheme proposed in this paper is based on well known feedforward techniques, used for decades in the communication industry mainly to cancel harmonic distortion in amplifiers (see e.g. [2], [3], [4]). The noise introduced by the amplifier is detected and subtracted at the output of the amplifier. Both the noise detection and the subtraction operations involve the amplitude of the noise sidebands, therefore affecting both phase and amplitude noise.

The limit of the cancellation ability of the scheme for short times depends only on the sensitivity of the noise detecting portion of the system. At long times, where thermal drifts come into play, the limits are set by the overall stability of all the system parameters and in particular of the noise subtraction point at the amplifier output.

II. THE NOISE CANCELLATION SYSTEM

Amplification of a signal is not a noiseless operation. All signal amplifiers, independent of the technology on which the device is based, introduce noise that may or may not degrade the quality of the signal undergoing amplification.

Such noise has both multiplicative and additive components. For a noiseless input signal $A\cos(\omega t)$ the result of the amplification process can be described as:

$$AG(1 + \hat{\epsilon}(t - \tau))\cos(\omega_0(t - \tau) + \hat{\phi}(t - \tau)) + G\hat{N}(t - \tau) \quad (1)$$

where G is the gain of the amplifier, τ is its time delay, $\hat{N}(t)$ is the additive input noise source, $\hat{\phi}(t)$ is the phase noise and $\hat{\epsilon}(t)$ is the amplitude noise, both due to multiplicative processes.

A. The conceptual scheme

A simplified noise cancellation scheme is drawn in Fig. 1. The *main amplifier* is shown with gain G and the *noise amplifier* with gain H . The relevant time delays introduced by various components are indicated with τ_i ($i=1,2,3,4$). The γ_i ($i=1,2$) are the coupling ratios of the directional couplers. A portion of the amplifier's input signal is compared, through a summing point (+), to a portion of the amplifier output signal. The time delays τ_1 and τ_2 are adjusted so that the result of the sum is the elimination of the carrier. The output of this sum ("sum" in Fig. 1) is then the noise introduced by the *main amplifier*.

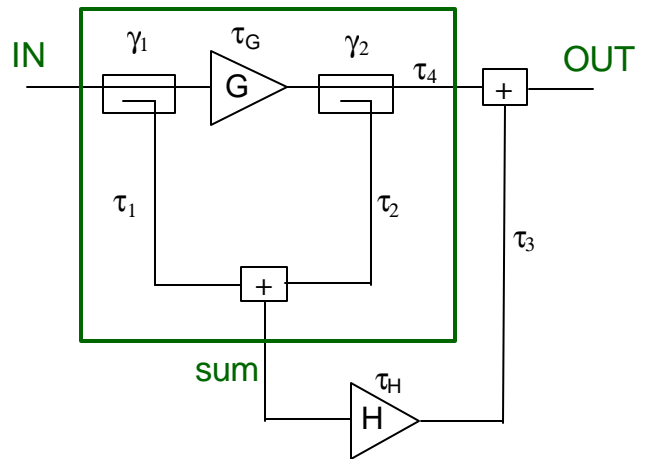


Fig. 1. Conceptual feedforward scheme for noise reduction. The amplifier with gain G is the *main amplifier*, while the other (gain H) is the *noise amplifier*. The relevant time delays introduced by various components are indicated with τ_i ($i=1,2,3,4$) and γ_i ($i=1,2$) are the coupling ratios of the directional couplers.

In particular, if the following conditions are met:

$$\begin{cases} \tau_2 + \tau_G = \tau_1 \pm \pi/\omega_0 \\ G\gamma_2 = \gamma_1 \end{cases} \quad (2)$$

then, at the output of the first summing point, perfect carrier cancellation is achieved, leaving only the noise (both amplitude and phase):

$$A\gamma_1[\hat{\phi}_G \sin(\omega_0(t-\tau)) - \hat{\epsilon}_G \cos(\omega_0(t-\tau))] - \gamma_1 \hat{N}_G(t-\tau) \quad (3)$$

where the subscript “G” indicates that the noise processes belong to the *main amplifier*, with gain G.

This result is then amplified with gain H and summed back to the output signal where, with the proper delay match, the noise is cancelled. The noise cancellation condition is:

$$\begin{cases} \tau_1 + \tau_H + \tau_3 = \tau_4 + \tau_G \\ \gamma_1 H = G \quad \text{or} \quad \gamma_2 H = 1 \end{cases} \quad (4)$$

and the result of it is:

$$OUT = AG \cos(\omega_0(t-\tau)) + H \hat{N}_H(t-\tau). \quad (5)$$

where \hat{N}_H is the additive noise associated with the second amplifier (*noise amplifier*).

It is apparent that both amplitude and phase noise introduced by the main amplifier have been cancelled.

The presence of the thermal noise \hat{N}_H determinates the ultimate limit of the system: in ideal conditions (perfect sums at both summing points) the thermal noise floor of the noise-canceling portion of the system sets the maximum amount of achievable noise cancellation. The perfect cancellation of the signal carrier before entering the *noise amplifier* minimizes the effect of multiplicative noise processes, limiting the noise contribution of the second amplifier to its additive component \hat{N}_H .

The important feature of the scheme is the ability to eliminate the multiplicative noise $\hat{\phi}_G$ introduced by the main amplifier. In fact, although it is possible to improve the signal-to-noise ratio by increasing the power of the carrier, when the amplifier noise has constant power spectral density (as it is for thermal noise), it is not true for amplifiers with $1/f$ noise behavior of the power spectral density. On the contrary, an increase in the carrier power at the input of the amplifier generates a larger amount of multiplicative noise at the output.

B. Effects of imperfect sums

The conditions (2) and (4) for perfect carrier and noise cancellation are likely to be imperfectly satisfied, due to delay and/or amplitude mismatches. Main causes of such imperfections are the sensitivity and the stability over time of the components used to meet the conditions. The imperfect version of condition (2) is:

$$\begin{cases} \tau_2 + \tau_G = \tau_1 + \Delta\tau_c \pm \pi/\omega_0 \\ G\gamma_2 = \gamma_1 + \Delta\alpha_c \end{cases} \quad (6)$$

where $\Delta\tau_c$ is the time delay mismatch and $\Delta\alpha_c$ is the amplitude mismatch at the first summing point. It is useful to remember that the mismatch terms ($\Delta\tau$, $\Delta\alpha$) and the noise terms ($\hat{\alpha}$, $\hat{\phi}$, \hat{N}) are all considered *small* so we can use linear expansions for trigonometric functions and neglect the higher order terms in these calculations. The mismatch terms and the noise terms are fundamentally different in that the former are deterministic quantities (which may include drifts) while the latter are stochastic quantities described by probability functions and/or spectral densities.

The result of the first summing point is:

$$\begin{aligned} \text{sum} = & A\gamma_1[\hat{\phi}_G \sin(\omega_0(t-\tau)) - \hat{\epsilon}_G \cos(\omega_0(t-\tau))] \\ & - \gamma_1 \hat{N}_G(t-\tau) + \text{residualcarrier} \end{aligned} \quad (7)$$

It contains the noise terms of (3) and a term that represents the residual uncanceled carrier:

$$\text{residualcarrier} = A(1 + \epsilon_G) \Delta\alpha_c \cos\left(\omega_0(t-\tau) + \gamma_1 \frac{\Delta\phi_c}{\Delta\alpha_c} + \hat{\phi}_G\right) \quad (8)$$

Continuing the analysis of the system in non-ideal conditions, we now look at the second summing point. The noise is subtracted from the main amplifier's output signal and condition (4) becomes:

$$\begin{cases} \tau_1 + \tau_H + \tau_3 = \tau_4 + \tau_G + \Delta\tau_n \\ \gamma_1 H = G + \Delta\alpha_n \end{cases} \quad (9)$$

where $\Delta\tau_n$ is the time mismatch and $\Delta\alpha_n$ is the amplitude mismatch. The system's output is:

$$\begin{aligned} OUT = & A \cdot G \cdot [1 + AM] \cos[\omega_0(t-\tau) + PM] \\ & + H \cdot \hat{N}_H(t-\tau) - \Delta\alpha_n \cdot \hat{N}_G(t-\tau) \end{aligned} \quad (10)$$

In addition to the noise terms in (5) we now have additional amplitude and phase multiplicative noise and some residual additive noise associated with the main amplifier. The additive noise associated with the *noise amplifier* (\hat{N}_H) is part of the output signal even in the case of ideal cancellation. The multiplicative noise terms are:

$$AM = \frac{\Delta\alpha_c}{\gamma_1} \cdot \hat{\epsilon}_H + \left(\frac{\Delta\alpha_c}{\gamma_1} - \frac{\Delta\alpha_n}{G} \right) \cdot \hat{\epsilon}_G + \Delta\phi_n \cdot \hat{\phi}_G \quad (11)$$

$$PM = \Delta\phi_c \cdot \hat{\epsilon}_H + (\Delta\phi_c - \Delta\phi_n) \cdot \hat{\epsilon}_G + \frac{\Delta\alpha_c}{\gamma_1} \cdot \hat{\phi}_H + \left(\frac{\Delta\alpha_c}{\gamma_1} - \frac{\Delta\alpha_n}{G} \right) \cdot \hat{\phi}_G$$

The following comments illustrate the meaning of (11). Both mismatches, at the first and second summing point, contribute to the noise term associated with the main amplifier. The presence of multiplicative noise generated by the *noise amplifier*, amplitude noise $\hat{\epsilon}_H(t)$ and phase

noise $\hat{\phi}_H(t)$, is caused by the mismatch at the first summing point. In fact, the presence of a residual carrier triggers multiplicative noise generation in the second amplifier (*noise amplifier*).

Furthermore, as expected from interferometer-type structures, a PM-AM conversion (and vice-versa AM-PM) generates a few more terms, due to mismatch at both summing points.

III. EXPERIMENTAL CHARACTERIZATION

A proof-of-concept system was built according to the scheme in Fig. 2. The variable phase shifters and attenuators indicated with α_c , α_n , Φ_c , and Φ_n are necessary to fulfill the cancellation conditions for the summing points SUM_1 and SUM_2 and were not shown in Fig. 1 for clarity.

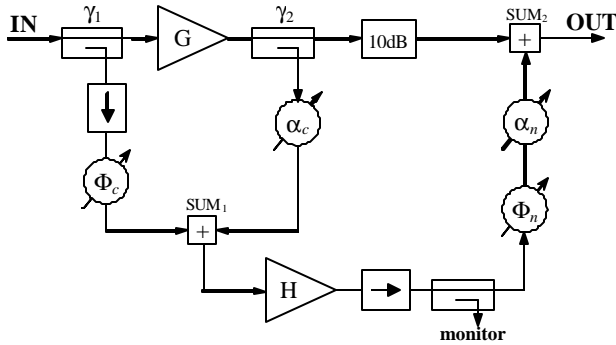


Fig. 2. Experimental setup for the proof-of-concept noise canceling system. The working frequency is about 10GHz.

The *main amplifier* is a medium-power microwave amplifier with gain $G = 33\text{dB}$ and 1-dB compression point at $P_{\text{out}} = +22\text{dBm}$, while the *noise amplifier* is a low-power amplifier with gain $H = 35\text{dB}$ and 1-dB compression point at $P_{\text{out}} = +15\text{dBm}$. The choice of these two components was determined only by availability. The first directional coupler is a Wilkinson power splitter so $\gamma_1 = 3\text{dB}$. The directional coupler at the output of the main amplifier has a coupling ratio of $\gamma_2 = -20\text{dB}$. The 10dB fixed attenuator is necessary only to balance the amplitudes at the output summing point (SUM_2) in the present (suboptimal) setup, since the *noise amplifier* gain is not high enough. All the variable attenuators and phase shifters are mechanical and cannot be servoed. The monitor port, with a coupling ratio of -20dB , allows the measurement of the residual carrier, amplified by the *noise amplifier*.

The measured phase noise of the *main amplifier* by itself is shown in Fig. 3, together with the results labeled “cancellation off” that were obtained from a phase noise measurement of the complete setup (Fig. 2) with α_n set to 30dB. The high value of α_n disables the noise cancellation at the output of the amplifier, as confirmed by the close agreement between the two measurements of Fig. 3. Turning up the attenuation α_n provides then a convenient reference for the evaluation of the amount of noise cancellation produced by this setup.

Upon balancing the phases and amplitudes at both summing points (SUM_1 and SUM_2), the residual phase noise of

the system is measured. Results are shown in Fig. 4, where the effect of the noise cancellation is apparent from the comparison of the case where the cancellation is “off” and the measured phase noise is that of the main amplifier alone. The net gain of the amplifier with the noise cancellation scheme, that is the ratio of P_{OUT} and P_{IN} (see Fig. 2), is $G_{\text{TOT}} = 21\text{dB}$, with an output power of $P_{\text{OUT}} = +11\text{dBm}$.

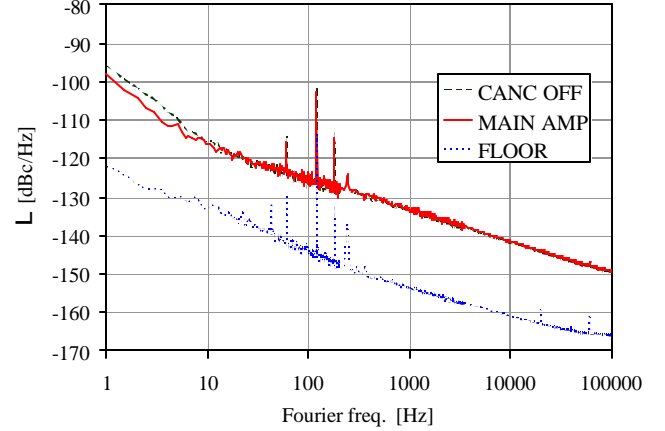


Fig. 3. Measured one-sided phase noise power spectral density $L(f)$ for the main amplifier with gain G (grey solid line). The amplifier is working in linearity (small signal conditions) and its phase noise is compared with the one measured for the complete system of Fig. 2 when α_n is maximized to about 30dB (black dashed line). With such attenuation there is practically no noise cancellation at the amplifier output (SUM_2).

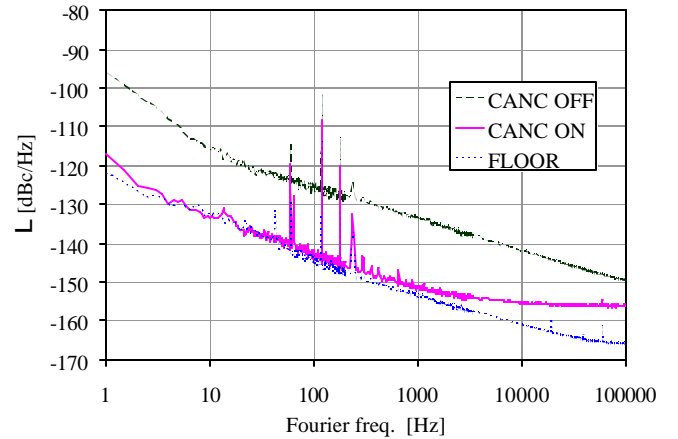


Fig. 4. Residual one-sided phase noise power spectral density $L(f)$ for the system depicted in Fig. 2 (grey solid line) compared with the measurement system noise floor (dotted line) and with the phase noise of the main amplifier alone (black dashed line, measured with “cancellation off”). The net gain of the system is 21dB with 11dBm of output power.

The amount of phase noise cancellation, taken from the results in Fig. 4, is summarized in Table 1 for decades offset frequencies starting at 1Hz.

1Hz	10Hz	100Hz	1kHz	10kHz	100kHz
21dB	17.3dB	18.5dB	17.8dB	13.7dB	6.8dB

Table 1. Results of the application of the noise cancellation scheme of Fig. 2 expressed in dB of difference between the one-sided phase noise power spectral densities measured with the cancellation “on” and “off”.

There are two fundamental limitations in the results of this implementation of the noise cancellation system, as can be inferred from Fig. 4. The first one comes from the measurement system noise floor (grey dotted line in Fig. 4) and it affects offset frequencies up to about 1kHz. The second one is the white noise plateau at higher offset frequencies and it is the additive noise associated with the noise amplifier, represented by the term $H \cdot \hat{N}_H$ in (5) and (10).

The present implementation of the cancellation scheme does not have the capability to control the phase and the amplitude balance at the summing points. Nonetheless it is possible to perform a qualitative estimation of the control system parameters, in particular the stability level needed to maintain the system performance. This has been done by comparing the results of two noise measurements performed at different times as shown in Fig. 5. The second measurement has been performed 45 minutes after the first one, without having compensated for the drift-caused unbalances at the summing points.

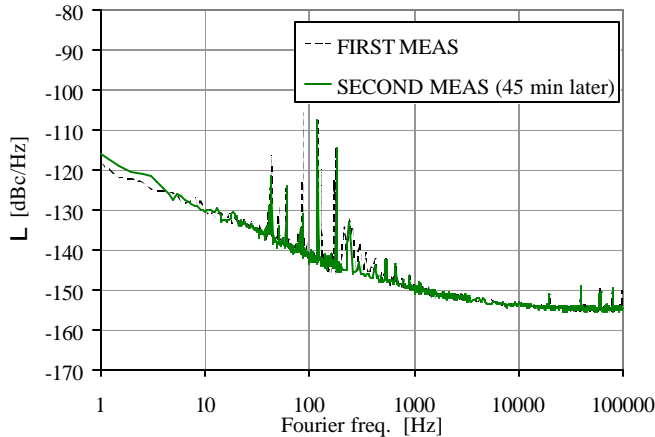


Fig. 5. Results of the phase noise measurements performed in order to qualitatively evaluate the stability characteristics (over time) of the cancellation scheme. The second measurement (grey solid line) has been performed 45 minutes after the first one (black dashed line) without compensating for the drift-caused unbalances in the summing points.

The very good agreement between the two subsequent measurements indicates that the degradation of the amplitude and phase balance for the canceling conditions at both summing points doesn't reduce the amount of noise cancellation.

Equation (10) clearly indicates that the residual multiplicative phase noise on the output signal is proportional to the unbalance at both summing points. The results in Fig. 5, however, are practically superimposed although the residual carrier has increased of about 10dB during the 45 minutes interval. This confirms (at least qualitatively) that the limit in the amount of noise cancellation shown in Fig. 4 is set by the measurement system noise floor, suggesting that larger amounts of multiplicative noise cancellation are already present in the system.

IV. SUMMARY

Preliminary results for a noise cancellation scheme based on a feedforward configuration have been presented, together with a first-order analysis of the different system noise sources. A qualitative study of the stability characteristics of the system is also provided, based on results of different measurements over a period of time.

ACKNOWLEDGMENTS

The authors would like to thank S. R. Jefferts for invaluable support and very constructive discussions.

REFERENCES

- [1] T. E. Parker, "Characteristic and sources of phase noise in stable oscillators," *Proceedings of the 41st IEEE Frequency Control Symposium*, pp. 99-110, 1987.
- [2] C. McNeilage, E. N. Ivanov, P. R. Stockwell, J. H. Searls, "Review of feedback and feedforward noise reduction techniques," *Proceedings of the IEEE Frequency Control Symposium*, pp. 146-155, 1998.
- [3] C. D. Broomfield, J. A. K. Everard, "Flicker noise reduction using GaAs microwave feedforward amplifiers," *Proceedings of the IEEE Frequency Control Symposium*, pp. 525-530, 2000.
- [4] P. B. Kenington, *High Linearity RF amplifier design*, Boston, Artech House, 2000.